This is a repository copy of *Genomics of altitude-associated wing shape in two tropical butterflies*.

White Rose Research Online URL for this paper:
https://eprints.whiterose.ac.uk/176631/

Version: Published Version

SPECIAL ISSUE

MOLECULAR ECOLOGY WILEY

Genomics of altitude-associated wing shape in two tropical butterflies

Gabriela Montejo-Kovacevich[1] | Patricio A. Salazar[2] | Sophie H. Smith[2] |
Kimberly Gavilanes[3] | Caroline N. Bacquet[3] | Yingguang Frank Chan[4] |
Chris D. Jiggins[1] | Joana I. Meier[1,5] | Nicola J. Nadeau[2]

[1]Department of Zoology, University of
Cambridge, Cambridge, UK

[2]Animal and Plant Sciences, University of
Sheffield, Sheffield, UK

[3]Universidad Regional Amazónica de
Ikiam, Tena, Ecuador

[4]Friedrich Miescher Laboratory of the
Max Planck Society, Tübingen, Germany

[5]St John's College, University of
Cambridge, Cambridge, UK

Correspondence
Gabriela Montejo-Kovacevich,
Department of Zoology, University of
Cambridge, Cambridge, UK.
Email: gmontejokovacevich@gmail.com

Nicola J. Nadeau, Animal and Plant
Sciences, University of Sheffield,
Sheffield, UK.
Email: n.nadeau@sheffield.ac.uk

Abstract

Understanding how organisms adapt to their local environment is central to evolution. With new whole-genome sequencing technologies and the explosion of data, deciphering the genomic basis of complex traits that are ecologically relevant is becoming increasingly feasible. Here, we studied the genomic basis of wing shape in two Neotropical butterflies that inhabit large geographical ranges. *Heliconius* butterflies at high elevations have been shown to generally have rounder wings than those in the lowlands. We reared over 1,100 butterflies from 71 broods of *H. erato* and *H. melpomene* in common-garden conditions and showed that wing aspect ratio, that is, elongatedness, is highly heritable in both species and that elevation-associated wing aspect ratio differences are maintained. Genome-wide associations with a published data set of 666 whole genomes from across a hybrid zone, uncovered a highly polygenic basis to wing aspect ratio variation in the wild. We identified several genes that have roles in wing morphogenesis or wing aspect ratio variation in *Drosophila* flies, making them promising candidates for future studies. There was little evidence for molecular parallelism in the two species, with only one shared candidate gene, nor for a role of the four known colour pattern loci, except for *optix* in *H. erato*. Thus, we present the first insights into the heritability and genomic basis of within-species wing aspect ratio in two *Heliconius* species, adding to a growing body of evidence that polygenic adaptation may underlie many ecologically relevant traits.

KEYWORDS
altitude, GWAS, *Heliconius*, local adaptation, polygenic, wing shape

1 | INTRODUCTION

Climate change is forcing organisms to "move, adapt, or die". With temperatures rising and land-use changing in the lowlands, shifting to higher elevations might be the only way to flee extinction for many taxa (Chen et al., 2011). However, the environment changes drastically along mountains, with diverse sets of challenges expected to drive local adaptation (Halbritter et al., 2015). Thus, identifying the genomic mechanisms that allow organisms to inhabit wide ranges is key to understanding which taxa are most likely to adapt locally when forced to colonise new, high-elevation, environments. With novel sequencing technologies and the explosion of genomic

data, we now have the tools to decipher the genetic basis of ecologically relevant traits in the wild.

Insect flight has many essential functions, including dispersal, courtship, and escaping predators (Dudley, 2002). As such, it is under strong selection to be optimised to suit local environments. Air pressure decreases with elevation, which in turn reduces lift forces required for taking flight, as well as oxygen available for respiration (Hodkinson, 2005). Subtle variation in wing morphology can have big impacts on flight mode and performance (Berwaerts et al., 2002). For example, butterflies in tropical rain forests have been found to have rounder wings when they inhabit the understory, both within closely related taxa (Chazot et al., 2014) and across many species (Mena et al., 2020). Elongated wings reduce wing-tip vortices, resulting in more efficient and faster flight, whereas short and wide wings are associated with higher manoeuvrability and lift (Le Roy et al., 2019a). Monarch butterflies have evolved two wing phenotypes: migratory populations have longer wings for long-distance gliding than those that remain year-round in Caribbean islands (Altizer & Davis, 2010). Thus, wing aspect ratio represents a trait probably undergoing strong selection across elevations and conferring local adaptation in insects.

Insect wing shape is phylogenetically conserved in many taxa (Houle et al., 2003; Montejo-Kovacevich et al., 2019; Thomas et al., 2000), but also highly evolvable in the laboratory (Houle et al., 2003), suggesting that it can be heritable. Experimental common-garden designs can help overcome the challenges of studying phenotypic clines in the wild and the effects of phenotypic plasticity, by providing the same environmental conditions to genotypes of different populations, which allows for the estimation of heritability (de Villemereuil et al., 2016). At the genetic level, wing morphogenesis has been mostly studied in *Drosophila*, with developmental pathways identified and many genes functionally tested (Carreira et al., 2011; Diaz de la Loza & Thompson, 2017; Pitchers et al., 2019). In other insects with wing dimorphisms, simple genetic architectures have been identified controlling wingless, or short winged, morphs (Li et al., 2020; McCulloch et al., 2019). However, studies describing the genetic basis of quantitative wing shape variation in organisms other than *Drosophila* are lacking.

Significant advances have been made in understanding the genetic basis of local adaptation in the wild. There are two general strategies to identify loci potentially under selection: (i) forward genetics, where known phenotypic traits are associated to genotypes (via genome-wide association studies or quantitative trait loci with laboratory crosses), and (ii) reverse genetics, where variation in allele frequencies in natural populations is studied to detect signatures of selection across the genome, without any prior knowledge of the phenotypes involved (Fuentes-Pardo and Ruzzante 2017; Pardo-Diaz et al., 2015). A good strategy is to study steep clines, where the environment changes continuously over a small space while gene flow is high, and combine both forwards and reverse genetics approaches (Cornetti & Tschirren, 2020; Tigano & Friesen, 2016). Sequencing individuals along such clines allows for sufficient phenotypic variance to measure and associate to genotypes (forward

genetics), while maintaining low genetic structure, and additionally test which genomic regions might be undergoing selection by comparing the extremes of the clines (reverse genetics). The study of aposematic wing pattern coloration in *Heliconius* butterflies is a prime example of this approach. Whole-genome sequencing in elevationally structured colour-morph hybrid zones has allowed for the identification of regions repeatedly differentiated across morphs and for each region to be associated via GWA studies with variation in specific patterns (Meier et al. 2021; Nadeau et al. 2014). Thus, population genetics across steep environmental clines or hybrid zones is a good approach to disentangle the genomic underpinnings of ecologically relevant traits.

Here we study the genetic basis of wing aspect ratio variation in two widespread species of *Heliconius* butterflies across an elevational cline in the Ecuadorian Andes. *Heliconius* inhabiting high altitudes have recently been found to have rounder wings than lowland butterflies, a pattern seen both across species and within species along elevational clines (Montejo-Kovacevich et al., 2019). To estimate the heritability of this potentially adaptive trait, we common-garden reared 71 broods of *H. erato lativitta* and *H. melpomene malleti* from across the cline, yielding 1141 offspring (Figure 1). We then used forward (GWAS) and reverse genetic approaches with whole-genome data of 666 of *H. erato* (n = 479) and *H. melpomene* (n = 187) individuals to identify regions associated with quantitative variation in wing aspect ratio and determined which regions diverged between extremes of the cline and had signatures of selective sweeps. This genomic data set was obtained from a study that developed a new low-cost linked-read sequencing technology, "haplotagging", to examine colour pattern clines in an altitudinally structured hybrid zone (Figure 1c, Meier et al. 2021). Here, we present the first study to examine the heritability and genomic basis of wing aspect ratio of two butterfly species in the wild.

2 | MATERIALS AND METHODS

2.1 | Study system and wild butterfly collection

H. erato and *H. melpomene* are the two most widespread *Heliconius* species, which diverged 12 million years ago and have Müllerian aposematic mimicry to advertise their toxicity to predators (Jiggins, 2016; Kozak et al., 2015). They can be found continuously coexisting across elevational clines ranging from sea level up to 1600 m along the Andean mountains. We sampled females of *H. erato lativitta* and *H. melpomene malleti* across the eastern slope of the Ecuadorian Andes for common-garden rearing (Figure 1b, orange triangles). For the genomic analyses we used a large data set from a nearby hybrid zone (Meier et al. 2021), where there are exclusively highland subspecies (*H. e. notabilis* and *H. m. plesseni*) that meet their respective lowland subspecies (*H. e. lativitta* and *H. m. malleti*) and mate freely within species, producing a stable intermediate wing pattern population (Figure 1c). *Heliconius* butterflies were collected with hand nets and precise location recorded. All detached wings were
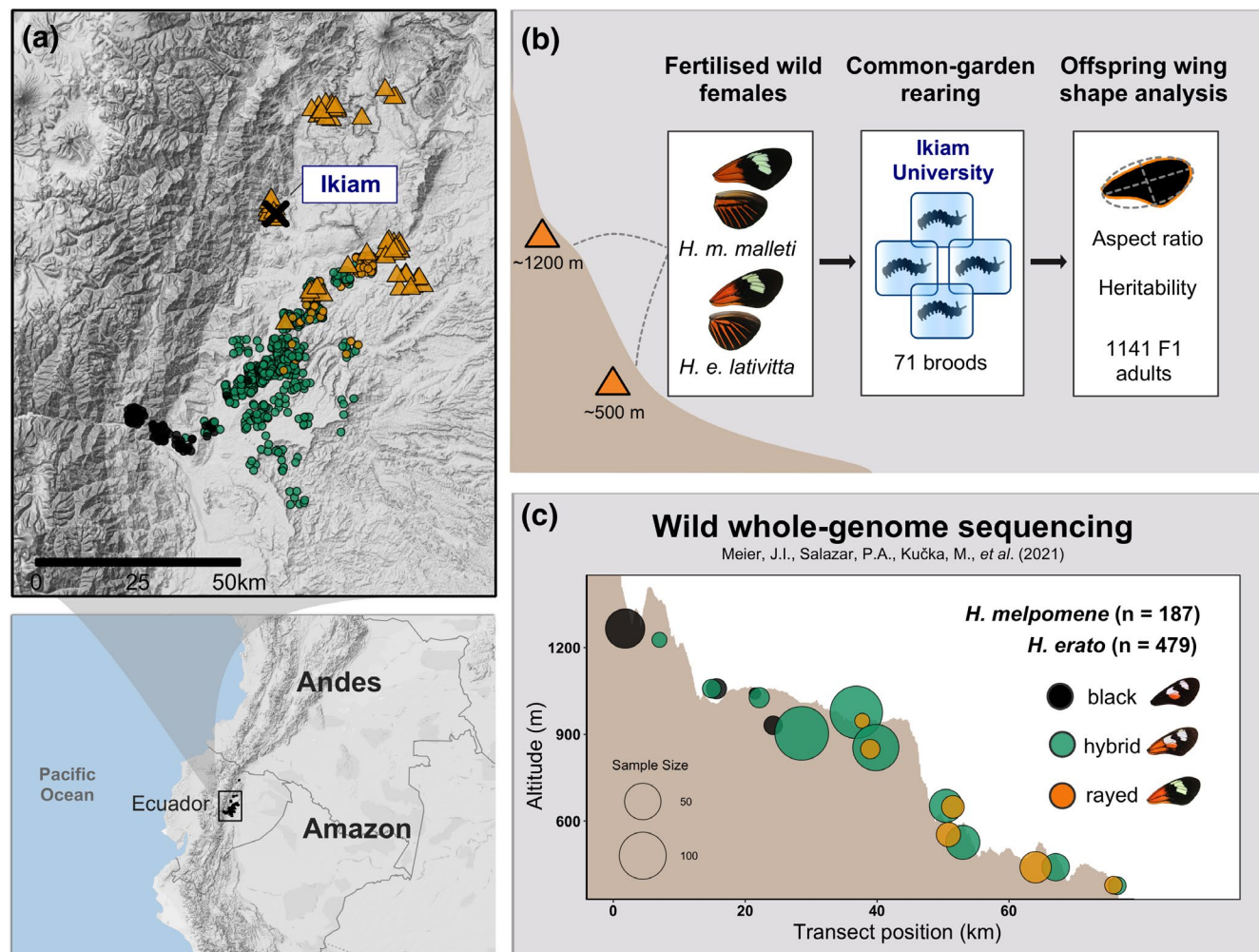
FIGURE 1 a) Each point represents an individual butterfly collected in the wild (triangles: females used for common garden rearing, circles: individuals whole genome-sequenced with haplotagging Meier et al. 2021). The cross highlights the positioning of the University of Ikiam, where the common-garden rearing took place. (b) Common-garden rearing protocol. (c) Topographic surface of transect across elevations used for whole-genome sequencing. Both species co-occur and have three main colour pattern morphs along this cline: two distinct colour pattern morphs (*H. e notabilis* and *H. m. plesseni*, referred to as "black", and *H. e lativitta* and *H. m. malleti*, referred to as "rayed") and within-species hybrids displaying admixed phenotypes (green circles), the most common hybrid phenotype is shown

photographed with a DSLR camera with a 100 mm macro-lens in standardised conditions, images and full records with data are stored in the EarthCape database (https://Heliconius.ecdb.io, Jiggins et al., 2019).

2.2 | Wing measurements

Wing morphology was analysed with an automated pipeline in the public software Fiji (Schindelin et al., 2012). Custom scripts automatically crop, extract the right or left forewing and perform particle analysis on the wing (Figure 1b). Wing area is estimated for the whole wing in mm^2. Wing aspect ratio is estimated by obtaining the best fitting ellipse of the same area as the wing, and obtaining the ratio between the major and minor axis' lengths. We only include forewings in this study, as they determine flight speed and mode, whereas hindwings act as an extended surface to support flight and

gliding (Le Roy et al., 2019b; Wootton, 2002), and they tend to be more damaged in *Heliconius* due to in-flight predation.

2.3 | Common garden rearing

Fertilised females of *H. erato lativitta* and *H. melpomene malleti* were caught in the wild at elevations ranging from 380 m up to 1600 m (Table S1). Females from all altitudes were simultaneously kept in separate 2 × 1 × 3 m cages of purpose-built insectaries at the Universidad Regional Amazónica Ikiam (Figure 1b. Tena, Ecuador, 615 m). Eggs were collected daily and individuals reared in separate containers throughout development in constant laboratory conditions (21.2 ± 1.1°C) between 2019–2020, except 10 families from *H. erato* which were reared in common outdoor insectary conditions in 2018. Offspring were individually fed the same host plants, *Passiflora punctata* for *H. erato* and *Passiflora edulis* for *H. melpomene*.

Development rates, pupal, and adult mass were recorded for all offspring.

2.4 | Whole genome data set

We used 666 whole-genomes of *H. erato* (*n* = 479) and *H. melpomene* (*n* = 187) from a recent study (Meier et al. 2021), sequenced with "haplotagging". This linked-read sequencing technique retains long-range information via barcoding of DNA molecules before sequencing, which permits megabase-size haplotypes to be computationally reconstructed (Meier et al. 2021). Linked-read sequencing (haplotagging) was performed to a mean read coverage of 1.54× and 2.77× (Meier et al. 2021). More details on analysis and phasing of molecules can be found in Meier et al. 2021, and summarised in the Supporting Information Materials (Note S1). The resulting data set used for analyses contained 25.4 million SNP positions for *H. erato* (66.3 SNPs/kbp) and 23.3 million for *H. melpomene* (84.7 SNPs/kbp).

2.5 | Statistical analyses

All nongenomic analyses were run in R V2.13 (R Development Core Team, 2011) and graphics were generated with the package ggplot2 (Ginestet, 2011). Packages are specified below and R scripts are publicly available (Zenodo https://doi.org/10.5281/zenodo.5060061). Sequence data from Meier et al. (2021) is deposited at the NCBI Short Read Archive (PRJNA670070).

2.5.1 | Effects of altitude on wing aspect ratio

To test the effects of maternal altitude on wing aspect ratio of common-garden reared offspring, we fitted a linear mixed model that included as fixed effects wing area, sex, development time (days from larva hatching until pupating), and altitude ("high" if the mother was collected ≥600 m.a.s.l.) with lme4 model fits (Bates et al., 2015). All continuous fixed effects were standardized to a mean of zero and unit variance to improve model convergence (Zuur et al., 2009). We included family ID as a random effect (intercept) to account for relatedness among offspring in *H. melpomene*. In *H. erato*, we nested family ID within experiment location as an additional random effect, as 10 of the families were reared in common-garden insectary conditions (2018), whereas the rest were reared in laboratory conditions (2019). We performed backward selection of random and fixed effects, in that order, with the package lmerTest (Kuznetsova et al., 2017), with likelihood ratio tests and a significance level of α = 0.1 (functions ranova() and drop1() Kuznetsova et al., 2017). When comparing models with different fixed effects we fitted maximum likelihood (REML = FALSE), otherwise restricted maximum likelihood models were fitted. Model residuals were checked for homoscedasticity and normality. With the coefficient of determination (R^2), we estimated the proportion of variance explained by the fixed factors

alone (marginal R^2, $R^2_{LMM(m)}$) and by both, the fixed effects and the random factors (conditional R^2, $R^2_{LMM(c)}$), implemented with the *MuMIn* library (Bartón, 2015; Nakagawa et al., 2017).

2.5.2 | Heritability estimates

To test the heritability of wing aspect ratio, we assessed wing aspect ratio variation across individuals from families reared in common-garden conditions. We used all broods with at least three offspring that could be phenotyped. First, we first used an ANOVA approach, with family identity as a factor explaining the variation in aspect ratio. We then estimated narrow-sense heritability (h^2) with two approaches (more details in Note S2). First, we estimated intraclass correlation coefficient (ICC) or repeatability (R) with a linear mixed model approach; family ID was set as the grouping factor, with a Gaussian distribution and 1000 parametric bootstraps to quantify uncertainty, implemented with the function rptGaussian() in the rptR package (Stoffel et al., 2017). Second, we estimated narrow-sense heritability (h^2) from the slope of mother and mid-offspring wing aspect ratio regressions for those families where the mother's wings were intact (31/48 broods in *H. erato* and 10/23 in *H. melpomene*).

2.5.3 | Genome-wide association mapping of wild wing aspect ratio

All population genomics analyses were performed in ANGSD version 0.933, which uses genotype likelihoods as input to account for genotype uncertainty and a Bayesian framework well-suited for large low-coverage sequencing data sets (Korneliussen et al., 2014). To account for population structure across the cline, we first calculated admixture proportions. We used a VCF with genotype likelihoods as input (Note S1) and ran NGSadmix (Skotte et al., 2013) on a random subset of 10% of the total sites with a minor allele frequency of at least 0.05. We specified two (*k* = 2) or three (*k* = 3) clusters for *H. erato* and *H. melpomene*, respectively, following Meier et al. (2021) who performed cluster selection with Clumpak (Kopelman et al., 2015).

To identify genomic regions potentially controlling quantitative wing aspect ratio variation in these two *Heliconius* species, we performed genome-wide association mapping (GWAS, doAsso ANGSD). VCF files from Meier et al. (2021) containing genotype likelihoods were used as input (-vcf-pl). We performed the GWAS with a generalized linear framework and a dosage model (-doAsso 6), which calculates the expected genotype from the input and implements a normal linear regression with the dosages as the predictor variable. Aspect ratio was used as the continuous response variable (-yQuant). Default filters were applied to remove sites with low heterozygosity (-minHigh 10) and with very low minor allele frequencies (-minCount 10). Three covariates were incorporated (-cov) to control for sex, wing area, and population structure with the admixture proportions obtained from NGSadmix, as described above. Likelihood ratio test

(LRT) statistics are calculated per site (following a chi-square distribution with one degree of freedom) under an additive model (-model 1) (Skotte et al., 2012).

In GWAS with fewer unlinked SNPs, those with strong associations can sometimes be found in isolation, that is, without flanking SNPs showing association, and assumed to be in linkage with the causal SNP. However, with large SNP data sets that are not pruned for LD, many are expected to show strong associations when located near the causal site or at random due to noise (Zhou et al., 2020). To partly account for this and facilitate the visualisation of regions with many associated SNPs, we obtained median and minima SNP association p-values for sliding windows of 50 SNP, with a step size of 10 SNP, with the R package "WindowScanR" (Tavares, 2016/2020). When visualising our results, we first use median p-value per window, plotted as $-\log10(p\text{-value})$, to regionally smooth the results so that spurious associations get dampened by their flanking high p-value SNPs, while regions with many SNPs with strong associations will be easily identifiable, as their median will remain high. This is analogous to recently developed methods for medical genetics that use penalized moving-window regressions (Bao & Wang, 2017; Begum et al., 2016; Braz et al., 2019; Chen et al., 2017) or LD clumping (Marees et al., 2018).

We generated a per SNP null distribution of p-values by repeating the genome-wide association analysis 200 times, with randomly permuted phenotypes (aspect ratios) in each run. To obtain a null distribution of p-values per window, we then computed median p-values of the same sliding windows as in the observed data set across the genome for all 200 permutations. Our final set of outliers only included windows that ranked above the 99th percentile of the window null distribution of p-values, that is, if the observed median p-value was the lowest or second lowest among the 200 median p-values obtained from permutations. We additionally performed "traditional" genome-wide thresholding by recording the lowest overall p-value and lowest window median p-value in each permutation and obtaining a critical p-value threshold at $p < .05$, to then assess if these outliers overlapped with our regions of interest. To check for outlier overlaps between species we mapped the *H. melpomene* windows (starts and end positions) to the *H. erato* reference genome using a chainfile from Meier et al. (2021) and the liftover utility (Hinrichs, 2006). Finally, to compare the distribution of outlier p-values in quantitative wing aspect ratio variation with a less polygenic trait, we additionally ran a GWAS with "red colour pattern" as a discrete phenotype (highland-like, hybrid-like, lowland-like).

2.5.4 | Identifying regions diverging between highland and lowland populations

We computed genetic differentiation (F_{ST}) between the highland and lowland subspecies (excluding the mid-elevation hybrids), to identify regions diverging across altitudes and potentially overlapping with wing aspect ratio associated regions. We calculated the site frequency spectrum (SFS) with genotype likelihoods for each population (dosaf, ANGSD). We then obtained folded 2D-SFS for both populations combined to use as a prior for the joint allele frequency probabilities with the function realsfs. F_{ST} was calculated per site using the Weir–Cockerham correction (realsfs F_{ST} index, ANGSD), and 5 kb window averages with 1 kb steps were obtained for plotting (following Meier et al. 2021). We additionally checked for overlaps between regions of interest and signatures of selective sweeps (obtained from Meier et al. 2021), such as reductions in nucleotide diversity differentiation between highland and lowland populations ($\Delta\Pi$), and high levels of intrapopulation integrated haplotype scores (iHS), which compare the levels of linkage disequilibrium surrounding the positively selected allele and those in the background allele at the same position (Szpiech & Hernandez, 2014).

2.5.5 | Candidate gene annotation

To study in depth some of the potentially many genes affecting wing aspect ratio, we examined regions that had at least one 50 SNP window with a median p-value below the threshold of $p < .01$ ($-\log10(p)_{median} > 2$), and 10 contiguous outlier windows (>99th percentile). We obtained the positions of the SNP with the strongest and second strongest association, to get the region with strongest association. We identified one gene if this region was within a gene, or the two closest genes if the region was intergenic or across two genes. We used reference genomes for both species stored in the genome browser Lepbase (Challis et al., 2016) to identify the genes (*H. erato* demophoon v.1; *H. melpomene* H. melpomene Hmel2.5), and extract the protein sequence. We then searched for similarity in protein sequence databases flybase, uniprotk, and ncbi, and present *Drosophila melanogaster* gene names in the main text and figures. Protein information, E-values, and GO-terms were recorded for each candidate. Additionally, we examined functional enrichment of all genes overlapping with any outlier window across the genome, which we present in the Supporting Information (Note S4).

3 | RESULTS

3.1 | Wing aspect ratio predictors and heritability

Wing aspect ratio was phenotyped in 721 *H. erato* offspring individuals from 48 full-sib families, and 419 individuals of *H. melpomene* from 23 full-sib families. Wing aspect ratio varied across families of both species (ANOVA: *H. erato* $F_{47, 673} = 3.93$, $p < .0001$, *H. melpomene* $F_{22, 396} = 11.9$, $p < .0001$). Offspring of highland *H. erato* mothers, on average, had rounder wings than those of lowland areas (Figure 2b, t test: *H. erato*: $t_{46b} = -3.5$, $p < .001$), whereas highland *H. melpomene* offspring were only marginally rounder than lowland families (Figure 2d; t test: $t_{20} = -2.02$, $p = 0.06$ and wing area did not differ across broods from different elevations (Figure S1C). Mean aspect ratio of broods recapitulated those found in wild specimens in a previous study (Figure S2; Montejo-Kovacevich et al., 2019).
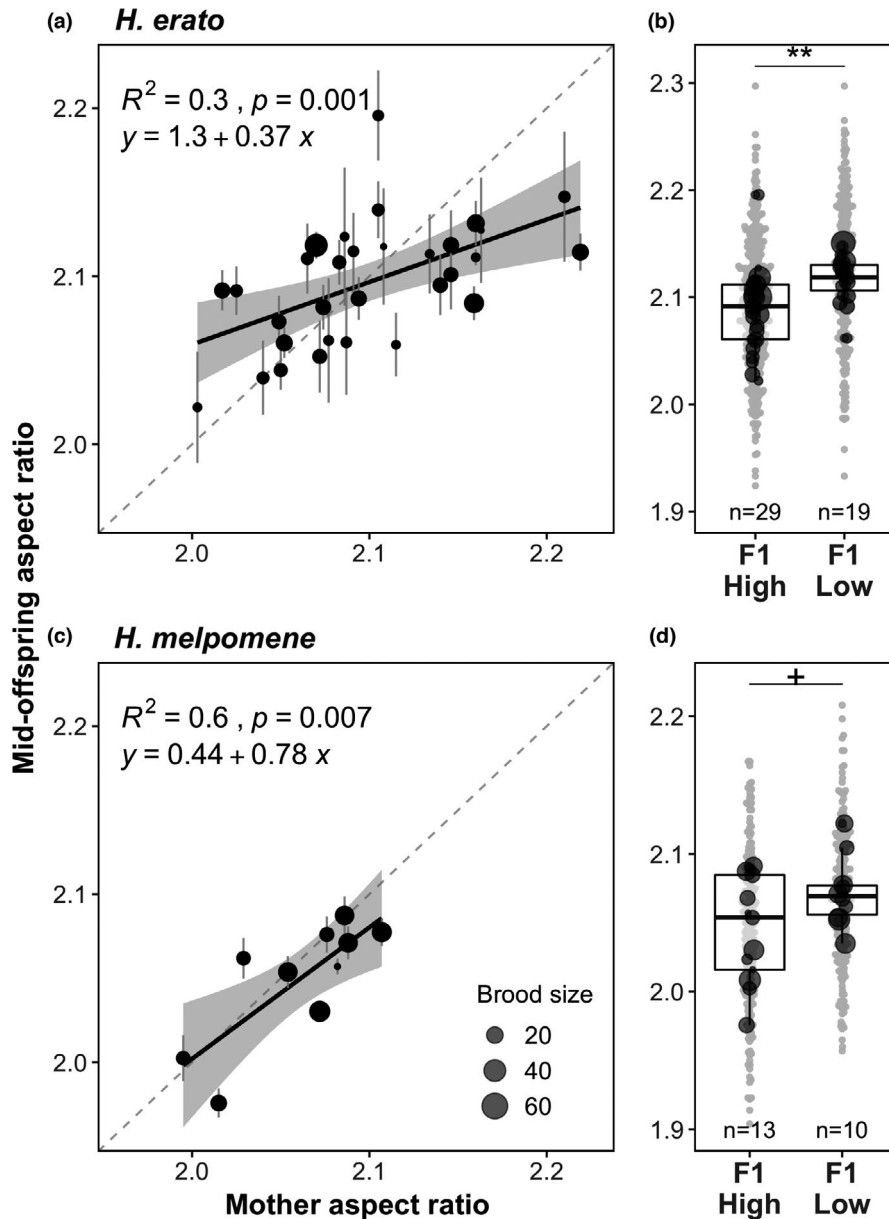
FIGURE 2 Mother and mid-offspring regression for wing aspect ratio (a,c) and F1 offspring wing aspect ratio with respect to maternal origin across elevations (b,d). Each black point represents mean wing aspect ratio per family and its size is proportional to number of offspring per family. Grey shading around the regression corresponds to 95% confidence intervals of the regression. Stars represent significance levels of two sample *t* tests between highland (≥600 m) and lowland (<600 m) family means for each species (+<0.075, *<.05, **<.01)

Altitude, wing area, development time, and sex were significant predictors of wing aspect ratio in common-garden reared individuals of *H. erato*, whereas *H. melpomene* offspring's wing aspect ratio was marginally explained by altitude, with sex and wing area having a stronger effect (Table 1). Of the variation in offspring wing aspect ratio, 15% and 38% was explained by family identity while accounting for significant fixed effects in *H. erato* (repeatability = 0.15, $SE = 0.04$, $p < .0001$) and *H. melpomene*, respectively (repeatability = 0.38, $SE = 0.08$, $p < .0001$), indicating heritability or maternal effects.

We obtained wing aspect ratios for all mothers that retained intact wings in captivity, totalling 31/48 broods of *H. erato*, and for 10/23 of *H. melpomene* broods. Mother and mid-offspring regressions showed strong correlations (Figure 2a,c), but heritability was lower in *H. erato* compared to *H. melpomene* (*H. erato*: slope = 0.37, $R^2 = 0.3$, $p = .001$; *H. melpomene*: slope = 0.79, $R^2 = 0.6$, $p = .007$). Due to the strong sexual wing aspect ratio dimorphism in *H. erato*

(Figure S3), mother-to-male offspring regressions had a higher intercept (Figure S4A). The high aspect ratio heritability observed in both species supports the study of its genomic basis.

3.2 | Genome-wide association mapping of aspect ratio variation

3.2.1 | Subspecies and hybrid phenotypes

Aspect ratio varied slightly across the elevational cline sampled for whole-genome sequencing of both species. Highland subspecies, *H. e. notabilis* and *H. m. plesseni* (black, Figure 3) were on average rounder than hybrids (green, Figure 3), i.e. with lower aspect ratios, and in *H. erato* they were also rounder than lowland subspecies *H. e. lativitta* (orange, Figure 3a). Hybrids did not differ in wing aspect ratio compared to their corresponding lowland subspecies, in other

TABLE 1 Wing aspect ratio linear mixed model summaries. Fixed effects are scaled and centred

Species	N	Random effects				Fixed effects (scaled)					
		Variable	Variance	SD	$R^2_{LMM(c)}$	Variable	Estimate	df	t-value	p-value	$R^2_{LMM(m)}$
H. erato	687	Mother ID (n = 48)	4.7e-04	0.022	0.33	Altitude (low)	0.029	37	3.52	<.001	0.21
		Residual	2.7e-04	0.052		Area	-0.008	526	-3.34	<.0001	
						Sex (male)	0.045	658	11.02	<.0001	
						Development time	-0.008	219	-2.88	<.01	
H. melpomene	419	Mother ID (n = 23)	1.0e-03	0.032	0.45	Altitude (low)	0.028	21.4	1.95	.06	0.11
		Residual	1.9e-03	0.043		Area	-0.010	410.3	-4.57	<.0001	
						Sex (male)	0.021	398.6	5.04	<.0001	
						Development time	0.004	319.5	1.01	n.s.	

Abbreviations: *df*, degrees of freedom based on Sattherwaithe's approximations. *p*, the *p*-values of fixed and random effects. Development time, time in days from larvae hatching to pupating. N, number of individuals with data for all fixed effects. Conditional R^2 values for models with fixed and random effects ($R^2_{LMM(c)}$), residual R^2 values fixed-effects only models ($R^2_{LMM(m)}$).

words, hybrids were phenotypically more lowland-like (Figure 3a). More importantly, the aspect ratio of hybrid individuals encompassed most of the trait variance of the pure subspecies (Figure S5), increasing our power to detect genomic associations. Migration and gene flow across the altitudinally-structured transect led to clinal variation in genome-wide admixture proportions between individuals (Figure S6; Meier et al. 2021).

3.2.2 | Association mapping of aspect ratio variation

Genome-wide association mapping for wing aspect ratio revealed many 50 SNP windows of high association (Figure 4). This suggests a highly polygenic basis, especially when compared to the effect size distribution of the red pattern phenotype association which is controlled by a single large-effect locus (Figures S7, S8). We obtained association statistics for 11.3 million SNPs (29.4 SNPs/kb) and 10.7 million SNPs (38.8 SNPs/kb) for *H. erato* and *H. melpomene*, respectively, from SNPs that passed the heterozygosity and minimum minor allele count filters. We found that certain genomic regions were strongly associated (Q–Q plots Figure S9, permutations Figure S10). Outlier 50 SNP windows were on average 1681 bp (background = 1641 bp) and 1273 bp (background = 1251 bp) long for *H. erato* and *H. melpomene*, respectively, and much smaller than the observed LD blocks (Figure S11). We further investigated 28 regions that had 10 adjacent outlier windows supported by permutations and had a median *p*-value <.01 (-log10(*p*)>2, Figure 4). In each species, one of these regions had SNPs above the genome-wide critical threshold (*p* < .05), and four (/12) and two (/16) for *H. erato* and *H. melpomene*, respectively, had median *p*-values above the window median *p*-value genome-wide critical threshold (*p* < .05; Figure S12).

3.2.3 | Candidate genes

To highlight candidates potentially controlling wing aspect ratio that could warrant further investigation, we identified genes in 28 regions of interest that had a high density of outlier SNPs, yielding 23 and 22 candidate genes for *H. erato* and *H. melpomene*, respectively. In 12 out of the 28 regions, SNPs within the region of strongest association were found within genes that could be annotated (Tables 2, 3). The remaining outliers were intergenic (n = 16) and potentially associated with regulatory variants, and were, on average, 35.8kb from the nearest (n = 6) or second nearest gene (n = 10, Tables 2, 3), that is, either upstream or downstream. The second nearest gene was presented in the main text if the closest gene was poorly annotated, or if it had a more relevant biological function, for example, known to affect wing aspect ratio or colour patterning in *Heliconius* (all genes in Table S1).

Several candidate genes, in both species, encoded proteins previously identified in *Drosophila* as involved in wing morphogenesis. The most relevant and functionally tested candidate genes of wing
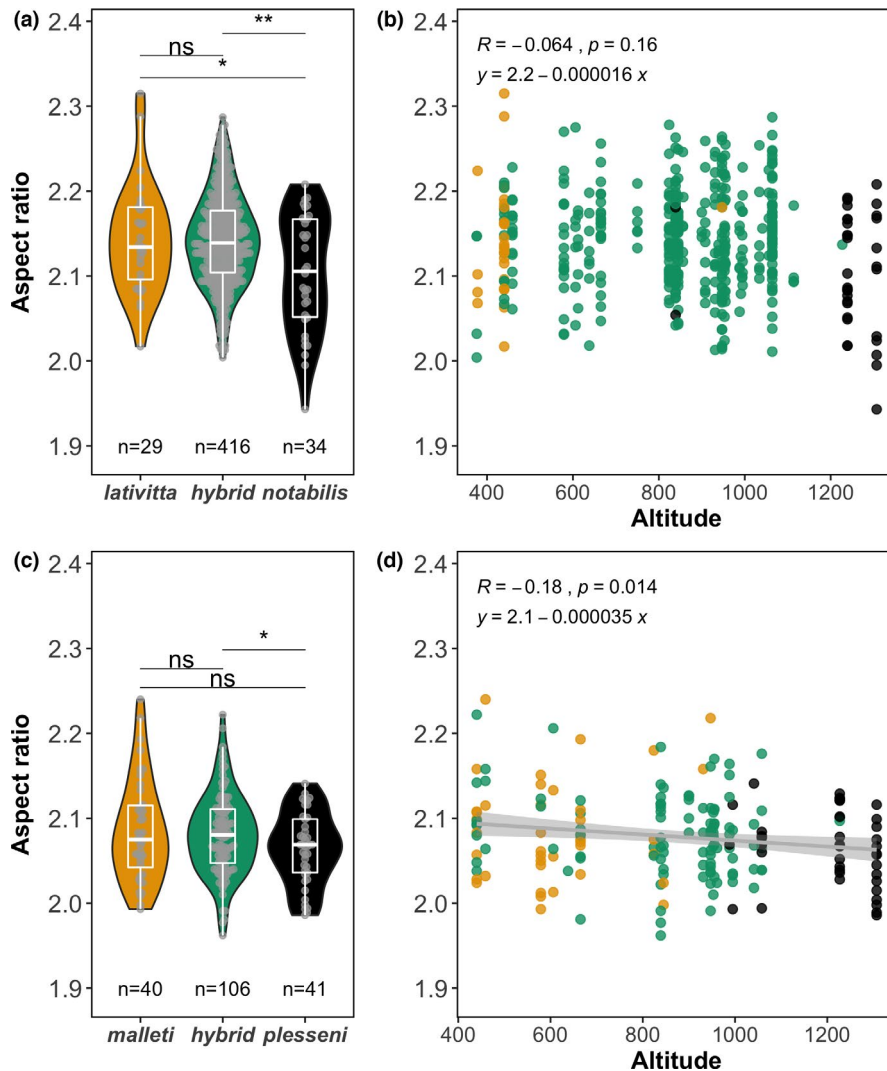
FIGURE 3 Phenotypes of whole-genome sequenced individuals included in the GWAS (*n* = 666). Wing aspect ratio across subspecies and altitudes of *H. erato* (a,b) and *H. melpomene* (c,d). Stars represent significance levels of two sample *t* tests between subspecies of each species (*<.05, **<.01)

aspect ratio variation were *su(dx)* in *H. erato*, and *dok*, *knrl*, *lowfat*, and *tap42* in *H. melpomene* (Figure 4, Tables 2, 3). Tracheal development and septate junction assembly functions were also associated with several candidates (*vari*, *pickle*, "pasi", *punch*, *pak1*, *knrl*), as well as chitin-based cuticule development (*punch*, *pgm2a* Pan et al., 2020), pigment transport or synthesis (*MCT9*, *optix*, *punch*, *ABCG*) and oxidative stress responses and regulation of cell apoptosis (*tefu*, *daxx*, *pak1*, *naam*). Some of these candidates, even if not directly involved in wing morphogenesis, have been functionally tested in *Drosophila* and lead to wing aspect ratio or wing vein abnormalities (*knrl* Lunde et al., 2003, *pgm2a* Pan et al., 2020, *tefu* Song et al., 2004, *daxx* Hwang et al., 2013). More importantly, 1/23 and 5/22 candidate genes in *H. erato* and *H. melpomene*, respectively, were direct enhancers or suppressors of genes recently identified as being involved with multivariate wing aspect ratio variation in *D. melanogaster* (Tables 2, 3; Pitchers et al., 2019; Thurmond et al., 2019).

We detected one case of possible parallelism between the two species on chromosome 13, with SNPs with the lowest *p*-values in both species mapping near the *rugose* gene, which affects neuromuscular junction development, synaptic architecture, brain morphology, and associative learning (Figure S13, Tables 2, 3. Wise et al.,

2015; Zhao et al., 2013). The epidermal growth factor receptor (*Egfr*) regulates *rugose* (Shamloula et al., 2002) and has been associated with wing aspect ratio variation in wild *D. melanogaster* (Dworkin et al., 2005) and, recently, in multivariate analyses of wing aspect ratio and knockdowns (Pitchers et al., 2019). In contrast, despite high levels of parallelism between species in the loci that control colour pattern differences across this hybrid zone (Figure S14, Meier et al. 2021), only one was significantly associated with wing aspect ratio variation in *H. erato*, the transcription factor controlling presence/absence of red, *optix* (Figure S13).

We found 39 and 23 significantly enriched GO-terms with genes overlapping with any outlier window across the genome in *H. erato* (Table S2) and *H. melpomene* (Table S3), respectively, seven of which were enriched in both species (Note S4, Figure S15). However, we found through simulations that genes overlapping GWAS hits are length biased, leading to certain categories being repeatedly enriched (Note S4, Figure S16, Figure S17). Categories most strongly enriched in the observed data set but not enriched in simulations included "actin filament organisation" in *H. erato* and "calcium ion transport" in *H. melpomene* (Tables S2, S3). Actin filaments have long been known to regulate butterfly wing scales (Dinwiddie et al.,
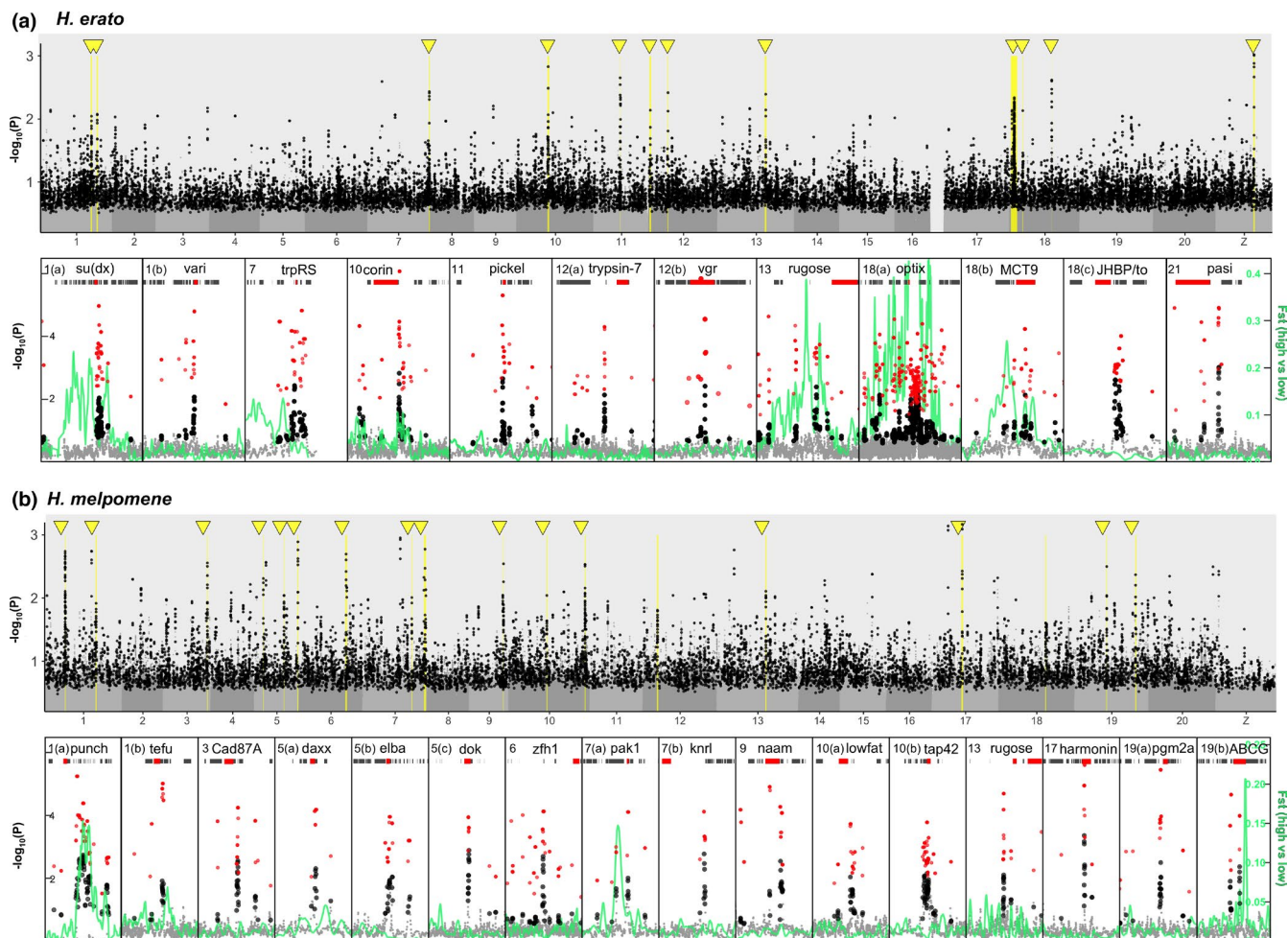
FIGURE 4 Genome wide association for wing aspect ratio in *H. erato* (a) and *H. melpomene* (b). Black points represent windows with *p*-values lower or equal to the top 1% of 200 permutations. Top panels for each species are manhattan plots of genome-wide associations, and bottom are zoomed-in regions of interest. In these regions, minimum *p*-values per outlier window are shown in red, gene tracks are shown as grey rectangles, selected genes within or near outlier regions are highlighted in red with gene abbreviations above them, and genetic differentiation between highland and lowland subspecies (excluding hybrids) along the region in green (F_{ST})

2014) and calcium ion channels are essential for wing development in Drosophila (George et al., 2019).

3.3 | Signatures of selection

To assess whether regions of interest identified in our association study presented signatures of positive selection at high altitude we used F_{ST} and nucleotide diversity differentiation between altitudes, as well as integrated haplotype scores (iHS, Figure S18). There is little background genomic differentiation between highland and lowland populations of both species (mean F_{ST} in *H. erato*: 0.0261 and in *H. melpomene*: 0.0189, Figure S14, Meier et al. 2021). Of the 28 regions identified as potentially associated with wing aspect ratio variation, nine were found to be in regions of elevated genomic differentiation between highland and lowland populations (≥3 standard deviations from the mean, F_{ST} green lines, Figure 4). Several regions of interest were also associated with negative differences

in nucleotide diversity between the highlands and the lowlands and with high integrated haplotype scores (Tables 2, 3; Figures S18, S19), both signatures of selective sweeps. The strongest four F_{ST} peaks in this cline are associated with colour patterning (Figure S14, Meier et al. 2021; Nadeau et al. 2014), but only *optix* (chr. 18) in *H. erato* was also strongly associated with wing aspect ratio (Figure S13).

4 | DISCUSSION

Here, we combine the power of hybrid zones across steep environmental clines, common garden rearing, and whole-genome sequencing to study the genomic basis of a potentially adaptive trait in the wild. We found that wing aspect ratio is highly correlated between mothers and their offspring in two butterfly species, highly repeatable across common-garden reared offspring families, and correlated with the altitude at which the mother was collected (Figure 2). With a large data set comprising

TABLE 2 *H. erato* candidate genes for regions of strong association with wing aspect ratio variation (*n* = 12). Genome-wide means: FST, 0.0261; iHShighlands, 0.054; iHSlowlands, 0.053. FST values ≥3 standard deviations from the mean are indicated by *ΔΠ(highlands-lowlands), 0.000662. References have been added for those candidate genes that have Drosophila mutants leading to wing aspect ratio changes. Candidate or related genes (†) identified in Pitchers et al. (2019) as significantly affecting multivariate wing aspect ratio in D. melanogaster are highlighted. Protein descriptions and relevant biological functions were extracted from Flybase (Thurmond et al., 2019), unless indicated otherwise

ROI	Gene ID	Distance (bp)	Abbrv.	Protein description	Relevant biological functions	Mutants in Dmel or GWAS outliers Pitchers(†)	Max. F_{ST}, min. $\Delta\Pi$	Max. iHS$_{hig}$ iHS$_{low}$
1a	Herato0101.595	within	**su(dx)**	E3 ubiquitin-protein ligase, suppressor of deltex	Wing disc dorsal/ventral pattern formation	Vein gaps, rounder wings (Mazaleyrat et al., 2003)	0.24*, −0.005	0.88, 0.25
1b	Herato0101.696	1567	vari	Membrane associated guanylate kinase	Septate junction morphogenesis, open tracheal system		0.08, −0.002	0.18, 0.2
7	Herato0701.777	within	trpRS	Tryptophan--trna ligase	Dendrite morphogenesis. Salivary gland.		0.15*, −0.003	0.72, 0.26
10	Herato1003.102	−3016	corin	Serine-type endopeptidase	Proteolysis		0.07*, 0	0.08, 0.16
11	Herato1108.269	2211	pickel, mega	Claudin transmembrane	Septate junction morphogenesis and function. Open tracheal system	Tracheal cell morphogenesis (Behr et al., 2003)	0.13, −0.002	0.44, 0.23
12a	Herato1201.11	60102	Trypsin-7	Trypsin-7. Serine-type endopeptidase	Proteolysis		0.07, −0.002	0.14, 0.27
12b	Herato1202.201	within	vgr	Vitellogenin receptor, yolkless	Oogenesis		0.06, −0.001	0.19, 0.12
13	Herato1301.557.1	68888	rugose	Neurobeachin	Neuromuscular junction, mushroom body, olfactory learning	Part of epidermal growth factor receptor (*EGFR* †) (Shamloula et al., 2002)	0.44*, −0.007	0.81, 0.25
18a	Herato1801.64	−131704	optix	Homeobox containing DNA binding protein	Red colour pattern *Heliconius*		0.96*, −0.018	0.97, 0.34
18b	Herato1801.138	within	MCT9	Monocarboxylate transporter 9, CG8468	Monocarboxylic acid transmembrane transporter		0.29*, −0.011	0.38, 0.12
18c	Herato1805.195	−2973	JHBP, takeout	Takeout-like, Juvenile Hormone Binding	Novel circadian output pathway, food status	Reduces male courtship behaviour (Dauwalder et al., 2002)	0.03, 0	0.17, 0.22
21	Herato2101.392	−24716	pasi	CG13288. Uncharacterized tetraspan.	Septate junction - Pasiflora1 (21% resemblance), (Deligiannaki et al., 2015)	Pasiflora1 mutant tracheal barrier breakdown (Deligiannaki et al., 2015)	0.06, 0	0.23, 0.21

Abbreviations: ROI, region of interest. Distance (bp) from gene to outlier window.

TABLE 3 *H. melpomene* candidate genes for ROI (n = 16). See Table 2 for details. Genome-wide means: FST, 0.0189; iHShighlands, 0.052; iHSlowlands, 0.053ΔΠ(highlands-lowlands), 0.000281

ROI	Gene ID	distance (bp)	Abbrv.	Protein description	Relevant Biological Functions	Mutants in Dmel or GWAS outliers Pitchers (†)	Max. F_{ST}, min. $\Delta\Pi$	Max. iHS_{hig} iHS_{low}
1a	HMEL014531g1	−13381	*punch*	Guanosine triphosphate cyclohydrolase 1	Larval chitin-based cuticle. Pteridine, melanin synthesis. Open tracheal system		0.15*, −0.004	0.5, 0.43
1b	HMEL011641g1	within	*tefu*	Serine/threonine-protein kinase ATM	DNA damage sensor, apoptosis, genotoxic stresses	Eye and wing abnormalities (Song et al., 2004)	0.07, −0.003	0.15, 0.13
3	HMEL017401g3	−3111	*cad87A*	Cadherin-87A-like	Calcium-dependent cell adhesion		0.03, −0.002	0.07, 0.12
5a	HMEL016253g1	within	*daxx*	Death domain-associated protein 6-like	Apoptosis, adult lifespan, oxidative stress	Small wings, locomotion (Hwang et al., 2013). suppressed by *foxo* †	0.05, −0.001	0.05, 0.06
5b	HMEL036769g1	within	*elba*	Early boundary activity protein 1-like	Embryonic development		0.03, 0	0.13, 0.17
5c	HMEL036887g1	within	**dok**	Insulin receptor substrate (IRS)	Imaginal disc-derived wing morphogenesis (Dok), neuromuscular synaptogenesis (Dok-7)	Shrivelled wings (Biswas et al., 2006)	0.06, −0.001	0.13, 0.06
6	HMEL037170g1	140607	*zfh1*	Zinc-finger homeodomain protein 1	Motor neuron axon		0.05, −0.001	0.07, 0.08
7a	HMEL016334g1	within	*pak1*	P21-activated protein kinase-interacting	Septate junction, synaptic development, epithelial morphogenesis, cell death	Photoreception, wings crumpled (Hing et al., 1999)	0.16*, −0.005	0.09, 0.14
7b	HMEL010451g1	−64775	**knrl**	Knirps-related. Transcription factors steroid hormones	Second wing vein, open tracheal system.	Second wing vein (Lunde et al., 2003). Regulates *knirps* †; enhanced by *kayak* †	0.04, −0.004	0.08, 0.19
9	HMEL009258g1	−594	*naam*	Putative pyrazinamidase/ nicotinamidase	Lifespan, neuron apoptosis, oxidative stress		0.02, −0.001	0.05, 0.07
10a	HMEL030728g1	−5022	**lft**	Lowfat, protein limb expression homolog. Fat/Dachsous, Frizzled	Imaginal disc-derived wing morphogenesis	Shorter wings (Mao et al., 2009). Enhances *fat* †	0.03, −0.001	0.1, 0.22
10b	HMEL009190g1	within	**TAP42**	Two A-associated protein of 42kda TAP42-like family, phosphatase inhibitor	Wing disc morphogenesis, mitotic spindle	Shriveled wings (Wang et al., 2012)	0.04, −0.001	0.25, 0.22
13	HMEL010907g1	65310	*rugose*	Neurobeachin-like	Neuromuscular junction, mushroom body, olfactory learning	Part of epidermal growth factor receptor (*EGFR* †) (Shamloula et al., 2002)	0.07, −0.003	0.22, 0.19
17	HMEL033852g1	within	*harmonin*	Putative harmonin, CG592.	Sensory perception of sound. Auditory organ (Li et al., 2018)		0.03, −0.001	0.08, 0.26
19a	HMEL002660g1	3416	*pgm2a*	Pgm2a phosphoglucomutase-2	Carbohydrate metabolism. Chitin synthesis plant hoppers, wing deformities (Pan et al., 2020)	*Pgm2b* †	0.05, −0.002	0.11, 0.18
19b	HMEL034862g1	within	*ABCG*	ATP-binding cassette subfamily G ABC transporter. CG5853	Metabolism (Wu et al., 2019)		0.23*, −0.002	0.1, 0.18

Abbreviations: ROI, region of interest. Distance (bp) from gene to outlier window.

666 whole-genomes sequenced with haplotagging (Meier et al. 2021) and association mapping, we uncover a highly polygenic basis to wing aspect ratio, and identify potential candidate genes in regions with many SNPs showing associations (Figure 4). Furthermore, with a population genetics approach, we find that many of these regions are also diverging between highland and lowland populations and some also overlap with signatures of selective sweeps, potentially being selected for local adaptation to highland environments.

4.1 | Wing aspect ratio is heritable

The amount of wing aspect ratio variation explained by family across common-garden reared offspring was high for both species (*H. erato*: 21% and *H. melpomene*: 39%), especially when compared to the 74% of variance explained by species identity in a previous comparative study (Montejo-Kovacevich et al., 2019). The resemblance in wing aspect ratio between mothers and their offspring is indicative of a highly heritable trait (Figure 2a), although we cannot rule out maternal effects partly driving this pattern. Rearing offspring in common-garden conditions strongly reduces the effects of shared mother-offspring environmental variables, but cannot account for, for example, variation in resources the mothers provide to their eggs. We found, however, that mother wing area did not correlate with offspring wing areas in *H. erato*, whereas it did in *H. melpomene* (Note S3). This highlights that wing aspect ratio might be less affected by maternal effects compared to other more condition-dependent traits, such as size. Furthermore, strong sexual dimorphism in wing aspect ratio present in *H. erato*, was maintained in common-garden reared individuals and both sexes had similar correlations with mother phenotypes, implying a strong genetic component to wing aspect ratio variation (Allen et al., 2011).

From a local adaptation perspective, we might predict wing aspect ratio to be highly heritable. Insects can behaviourally compensate for damaged or abnormal wings through changes in flight and body kinematics (Fernández et al., 2017). Yet, this might incur a fitness cost, as many behaviours, such as courtship and predator escape, are dependent on efficient flight (Le Roy et al., 2019a). Generally, cases of wing aspect ratio plasticity are rarer than size plasticity, especially if the two traits are allometrically decoupled, allowing for subtle changes to be selected if advantageous (Carreira et al., 2011; Gilchrist & Partridge, 2001; Strauss 1990). In *Heliconius*, wings have been found to be rounder at higher elevations, both across and within species that inhabit large ranges (Montejo-Kovacevich et al., 2019). In our study, wing aspect ratio differences observed in the wild in *H. erato* and *H. melpomene* were maintained in common-garden reared broods, with individuals from highland mothers having, on average, rounder wings (Figure 2b, Figure S2). Together, this supports the hypothesis that subtle changes in wing aspect ratio are highly heritable, and may be involved in local adaptation to altitude.

4.2 | Candidate genes associated with wing aspect ratio

We found 5/28 regions mapping to genes involved in the biological process of "wing disc development" and one involved in wing vein formation (Lunde et al., 2003). In *H. erato*, the most promising candidate gene was the suppressor of deltex, *su(dx)* (Figure 4a, Table 2), an E3 ubiquitin-protein ligase of the Notch signalling pathway (Jennings et al., 2007). *su(dx)* knockouts in *D. melanogaster* result in rounder wings via reduction of longitudinal wing venation (Mazaleyrat et al., 2003), wing margin reduction (Wilkin et al., 2004) or via interactions with other proteins (Djiane et al., 2011). Interestingly, this region has moderately high levels of genetic differentiation across high and low elevation populations ($F_{STmax} = 0.24$, Figures 4a, 1(a)), negative $\Delta\Pi$ (difference in nucleotide diversity), and very high integrated haplotype score in the highland population (0.88), which points towards altitude-associated selection on this candidate gene. In *H. melpomene*, we found four regions with genes functionally known to be involved in determining wing shape in *Drosophila* (Figure 4b, Table 3). Mutants of *lowfat* have shorter, rounder wings in *Drosophila* (Hogan et al., 2011; Mao et al., 2009), whereas *dok* mutants have shrivelled wings (Biswas et al., 2006). The knirps-related protein (*knrl*) is involved in second wing vein development (Table 3, Lunde et al., 2003), and *Tap42* (Figure 4b) triggers apoptosis in the developing wing discs (Wang et al., 2012). Thus, we have identified some promising genes that could be studied further in this system in future.

Despite phenotypic convergence towards rounder wings at high altitude, we found little evidence for molecular parallelism underlying wing aspect ratio variation between *H. erato* and *H. melpomene*. One of the 28 regions identified as potentially involved with this trait was found in the regulatory region of the gene rugose in both species (Figure S13). *Rugose* mutants also exhibit the "rough eye phenotype", aberrant associative odour learning, changes in brain morphology, and increased synapses in the larval neuromuscular junction (Shamloula et al., 2002; Volders et al., 2012). Furthermore, there was clear evidence of a selective sweep in this region in the highland *H. erato notabilis* (iHS, Table 2; Figures S18, S19). Interestingly, in *H. melpomene* a 4.8MB inversion was detected encompassing the rugose region (Meier et al. 2021). Inversions can aid local adaptation by retaining multiple co-adapted SNPs together (Mérot et al., 2020) but can also complicate GWA studies by causing large blocks of association that prevent the detection of causative SNPs or genes. The window approach we took could cause a bias toward such low-recombination regions, but this was the only one of our regions of interest to overlap with an inversion, out of the 33 detected for both species in Meier et al. (2021). In addition, the associations that we see are localised upstream of *rugose* and do not span the entire inversion, which is only present in *H. melpomene*. Thus, this region may be affecting aspect ratio in both species and under selection at high altitude, warranting future study.

In contrast, we found a strong association with wing aspect ratio variation at the *optix* locus uniquely in *H. erato*, which controls most

of the red colour patterning (Bainbridge et al., 2020; Lewis et al., 2019; Meier et al. 2021; Van Belleghem et al., 2017). Mimicry can play a role in *Heliconius*' wing shape, for example, morphs of *H. numata* that mimic the distantly related genus *Melinea* tend to converge in wing aspect ratios where they coexist (Jones et al., 2013). Although *H. erato* and *H. melpomene* mimic each other across their range and both have rounder wings in the highlands, the differences in aspect ratio between the two species are larger than those across elevations (Figure 3d). Thus, while some mimicry-related wing aspect ratio variation may be controlled by *optix*, many other loci are probably involved in shaping wings to suit the local environment and life-history of each species.

4.3 | Genetics basis of an ecologically relevant trait

A common criticism of population genomics approaches, reverse genetics, that aim to link genotypes and environments is that they often lack phenotypes. Traits directly measured from the wild might be a result of phenotypic plasticity, and are thus rarely used to infer local adaptation. Common-garden rearing can bridge the gap between phenotypes, genotypes, and environment, by providing measurements of heritability and repeatability of a trait across families whose genetic material comes from different extremes of an environmental cline (de Villemereuil et al., 2016). On the other hand, using highly differentiated populations can result in spurious phenotypic associations and makes identifying divergent outliers challenging. Thus, GWAS in the wild should use randomly mating populations with little population structure, while ensuring there is enough phenotypic variation to detect genetic associations with the trait of interest. Hybrid zones, where closely related subspecies or morphs come into contact along an environmental cline, can provide such ideal conditions to carry out GWAS in the wild.

Here, we have demonstrated the value of combining these approaches to gain insight into the genomic basis of an ecological relevant trait in the wild. We found that wing aspect ratio is highly heritable in two widespread species of *Heliconius* butterflies, and that altitude explains part of the variation in this trait. We have identified several regions potentially shaping wings in *H. erato* and *H. melpomene*, including five candidate genes involved in wing morphogenesis and several identified to be affecting wing aspect ratio in recent *Drosophila* studies (Pitchers et al., 2019). We found evidence of molecular parallelism between species and selective sweeps at high altitude at the gene *rugose*, and a strong association of *H. erato* wing aspect ratio with a known colour pattern locus, *optix*. Our study adds to a growing body of evidence showing that most quantitative traits conferring local adaptation are highly polygenic (Barghi et al., 2020). Spatial environmental heterogeneity and gene flow are thought to maintain high levels of standing genetic variation (Tigano & Friesen, 2016). This can favour polygenic adaptation, so that incomplete sweeps of many redundant loci can shift traits towards an optimum (Yeaman, 2015). A slow-moving optimum, such as range-expansions towards the highlands, should favour polygenic adaptation via small-effect loci, whereas selection for a distant optimum, such as a switch in colour pattern mimicry in *Heliconius*, should favour large-effect loci (Barghi et al., 2020). New whole-genome sequencing technologies could foster the study of local adaptation to the environment and shape our understanding of the mode and tempo of evolution in the wild.

AUTHOR CONTRIBUTIONS

Gabriela Montejo-Kovacevich, Patricio A. Salazar, Yingguang Frank Chan, Chris D. Jiggins, Joana I. Meier, Nicola J. Nadeau designed the study. Gabriela Montejo-Kovacevich, Patricio A. Salazar, Sophie H. Smith, Kimberly Gavilanes, Caroline N. Bacquet, Nicola J. Nadeau, performed the experiments and fieldwork. Gabriela Montejo-Kovacevich, Patricio A. Salazar, Yingguang Frank Chan, Joana I. Meier contributed to the analyses. Gabriela Montejo-Kovacevich wrote the first draft of the manuscript, all authors contributed to the final version.

OPEN RESEARCH BADGES

This article has earned an Open Data Badge for making publicly available the digitally-shareable data necessary to reproduce the reported results. The data is available at https://doi.org/10.5281/zenodo.5060061 and https://heliconius.ecdb.io/ [Jiggins et al., 2019].

DATA AVAILABILITY STATEMENT

All data and scripts are available have been made available in the public repository Zenodo (https://doi.org/10.5281/zenodo.5060061). Sequence data from Meier et al. (2021) is deposited at the NCBI Short Read Archive (PRJNA670070). All images and data associated to the individuals used for this study are available in the *Heliconius* Earthcape database (https://heliconius.ecdb.io/, Jiggins et al., 2019).

ORCID

Gabriela Montejo-Kovacevich https://orcid.org/0000-0003-3716-9929

Patricio A. Salazar https://orcid.org/0000-0001-8988-0769

Sophie H. Smith https://orcid.org/0000-0001-9530-3896

Caroline N. Bacquet https://orcid.org/0000-0002-1954-1806

Yingguang Frank Chan https://orcid.org/0000-0001-6292-9681

Chris D. Jiggins https://orcid.org/0000-0002-7809-062X

Joana I. Meier https://orcid.org/0000-0001-7726-2875

Nicola J. Nadeau https://orcid.org/0000-0002-9319-921X

REFERENCES

Allen, C. E., Zwaan, B. J., & Brakefield, P. M. (2011). Evolution of sexual dimorphism in the Lepidoptera. *Annual Review of Entomology*, https://doi.org/10.1146/annurev-ento-120709-144828.

Altizer, S., & Davis, A. K. (2010). Populations of monarch butterflies with different migratory behaviors show divergence in wing morphology. *Evolution*, *64*(4), 1018–1028. https://doi.org/10.1111/j.1558-5646.2009.00946.x.

Bainbridge, H. E., Brien, M. N., Morochz, C., Salazar, P. A., Rastas, P., & Nadeau, N. J. (2020). Limited genetic parallels underlie convergent evolution of quantitative pattern variation in mimetic butterflies [Preprint]. *Journal of Evolutionary Biology*, *33*(11), 1516–1529.

Bao, M., & Wang, K. (2017). Genome-wide association studies using a penalized moving-window regression. *Bioinformatics*, *33*(24), 3887–3894. https://doi.org/10.1093/bioinformatics/btx522.

Barghi, N., Hermisson, J., & Schlötterer, C. (2020). Polygenic adaptation: A unifying framework to understand positive selection. *Nature Reviews Genetics*, *21*(12), 769–781. https://doi.org/10.1038/s41576-020-0250-z.

Barton, K., & Barton, M. K. (2015). Package 'mumin'. *Version*, *1*(18), 439.

Bates, D., Mächler, M., Bolker, B., & Walker, S. (2015). Fitting linear mixed-effects models using lme4. *Journal of Statistical Software*, *67*(1), 1–48. https://doi.org/10.18637/jss.v067.i01.

Begum, F., Sharker, M. H., Sherman, S. L., Tseng, G. C., & Feingold, E. (2016). Regionally smoothed meta-analysis methods for GWAS datasets. *Genetic Epidemiology*, *40*(2), 154–160. https://doi.org/10.1002/gepi.21949.

Behr, M., Riedel, D., & Schuh, R. (2003). The Claudin-like megatrachea is essential in septate junctions for the epithelial barrier function in Drosophila. *Developmental Cell*, *5*(4), 611–620. https://doi.org/10.1016/S1534-5807(03)00275-2.

Berwaerts, K., Van Dyck, H., & Aerts, P. (2002). Does flight morphology relate to flight performance? An experimental test with the butterfly *Pararge aegeria*. *Functional Ecology*. https://doi.org/10.1046/j.1365-2435.2002.00650.x.

Biswas, R., Stein, D., & Stanley, E. R. (2006). Drosophila Dok is required for embryonic dorsal closure. *Development*, *133*(2), 217–227. https://doi.org/10.1242/dev.02198.

Braz, C. U., Taylor, J. F., Bresolin, T., Espigolan, R., Feitosa, F. L. B., Carvalheiro, R., Baldi, F., de Albuquerque, L. G., & de Oliveira, H. N. (2019). Sliding window haplotype approaches overcome single SNP analysis limitations in identifying genes for meat tenderness in Nelore cattle. *BMC Genetics*, *20*(1), 1–12. https://doi.org/10.1186/s12863-019-0713-4.

Carreira, V. P., Soto, I. M., Mensch, J., & Fanara, J. J. (2011). Genetic basis of wing morphogenesis in Drosophila: Sexual dimorphism and non-allometric effects of shape variation. *BMC Developmental Biology*, *11*(1), 32. https://doi.org/10.1186/1471-213X-11-32.

Challis, R. J., Kumar, S., Dasmahapatra, K. K., Jiggins, C. D., & Blaxter, M. (2016). *Lepbase: The Lepidopteran genome database* [Preprint]. *Bioinformatics*, https://doi.org/10.1101/056994.

Chazot, N., Willmott, K. R., Santacruz Endara, P. G., Toporov, A., Hill, R. I., Jiggins, C. D., & Elias, M. (2014). Mutualistic mimicry and filtering by altitude shape the structure of andean butterfly communities. *The American Naturalist*, *183*(1), 26–39. https://doi.org/10.1086/674100.

Chen, C., Steibel, J. P., & Tempelman, R. J. (2017). Genome-wide association analyses based on broadly different specifications for prior distributions, genomic windows, and estimation methods. *Genetics*, *206*(4), 1791–1806. https://doi.org/10.1534/genetics.117.202259.

Chen, I-C., Hill, J. K., Ohlemüller, R., Roy, D. B., & Thomas, C. D. (2011). Rapid range shifts of species associated with high levels of climate warming. *Science*, *333*(6045), 1024–1026. https://doi.org/10.1126/science.1206432.

Cornetti, L., & Tschirren, B. (2020). Combining genome-wide association study and FST-based approaches to identify targets of Borrelia-mediated selection in natural rodent hosts. *Molecular Ecology*, *29*(7), 1386–1397. https://doi.org/10.1111/mec.15410.

Dauwalder, B., Tsujimoto, S., Moss, J., & Mattox, W. (2002). The Drosophila takeout gene is regulated by the somatic sex-determination pathway and affects male courtship behavior. *Genes & Development*, *16*(22), 2879–2892. https://doi.org/10.1101/gad.1010302.

de Villemereuil, P., Gaggiotti, O. E., Mouterde, M., & Till-Bottraud, I. (2016). Common garden experiments in the genomic era: New perspectives and opportunities. *Heredity*, *116*(3), 249–254. https://doi.org/10.1038/hdy.2015.93.

Deligiannaki, M., Casper, A. L., Jung, C., & Gaul, U. (2015). Pasiflora proteins are novel core components of the septate junction. *Development*, *142*(17), 3046–3057. https://doi.org/10.1242/dev.119412.

Diaz de la Loza, M. C., & Thompson, B. J. (2017). Forces shaping the Drosophila wing. *Mechanisms of Development*, *144*, 23–32. https://doi.org/10.1016/j.mod.2016.10.003.

Dinwiddie, A., Null, R., Pizzano, M., Chuong, L., Krup, A. L., Tan, H. E., & Patel, N. H. (2014). Dynamics of F-actin prefigure the structure of butterfly wing scales. *Developmental Biology*, *392*(2), 404–418. https://doi.org/10.1016/j.ydbio.2014.06.005.

Djiane, A., Shimizu, H., Wilkin, M., Mazleyrat, S., Jennings, M. D., Avis, J., Bray, S., & Baron, M. (2011). Su(dx) E3 ubiquitin ligase–dependent and –independent functions of Polychaetoid, the Drosophila ZO-1 homologue. *The Journal of Cell Biology*, *192*(1), 189–200. https://doi.org/10.1083/jcb.201007023.

Dudley, R. (2002). The biomechanics of insect flight: Form, function, evolution. *Annals of the Entomological Society of America*, *93*(5), 1195–1196. https://doi.org/10.1093/aesa/93.5.1195f.

Dworkin, I., Palsson, A., & Gibson, G. (2005). Replication of an Egfr-Wing shape association in a wild-caught cohort of *Drosophila melanogaster*. *Genetics*, *169*(4), 2115–2125. https://doi.org/10.1534/genetics.104.035766.

Fernández, M. J., Driver, M. E., & Hedrick, T. L. (2017). Asymmetry costs: Effects of wing damage on hovering flight performance in the hawkmoth *Manduca sexta*. *Journal of Experimental Biology*, *220*(20), 3649–3656. https://doi.org/10.1242/jeb.153494.

Fuentes-Pardo, A. P., & Ruzzante, D. E. (2017). Whole-genome sequencing approaches for conservation biology: Advantages, limitations and practical recommendations. *Molecular Ecology*, *26*(20), 5369–5406. https://doi.org/10.1111/mec.14264.

George, L. F., Pradhan, S. J., Mitchell, D., Josey, M., Casey, J., Belus, M. T., & Bates, E. A. (2019). Ion channel contributions to wing development in *Drosophila melanogaster*. *G3: Genes, Genomes, Genetics*, *9*(4), 999–1008.

Gilchrist, A. S., & Partridge, L. (2001). The contrasting genetic architecture of wing size and shape in *Drosophila melanogaster*. *Heredity*, *86*(2), 144–152. https://doi.org/10.1046/j.1365-2540.2001.00779.x.

Ginestet, C. (2011). ggplot2: Elegant Graphics for Data Analysis. *Journal of the Royal Statistical Society: Series A (Statistics in Society)*, *174*(1), 245–246. https://doi.org/10.1111/j.1467-985X.2010.00676_9.x.

Halbritter, A. H., Billeter, R., Edwards, P. J., & Alexander, J. M. (2015). Local adaptation at range edges: Comparing elevation and latitudinal gradients. *Journal of Evolutionary Biology*, 28(10), 1849–1860. https://doi.org/10.1111/jeb.12701.

Hing, H., Xiao, J., Harden, N., Lim, L., & Zipursky, S. L. (1999). Pak functions downstream of dock to regulate photoreceptor axon guidance in Drosophila. *Cell*, 97(7), 853–863. https://doi.org/10.1016/S0092-8674(00)80798-9.

Hinrichs, A. S. (2006). The UCSC genome browser database: Update 2006. *Nucleic Acids Research*, 34(90001), D590–D598. https://doi.org/10.1093/nar/gkj144.

Hodkinson, I. D. (2005). Terrestrial insects along elevation gradients: Species and community responses to altitude. *Biological Reviews of the Cambridge Philosophical Society*, 80(3), 489–513. https://doi.org/10.1017/S1464793105006767.

Hogan, J., Valentine, M., Cox, C., Doyle, K., & Collier, S. (2011). Two frizzled planar cell polarity signals in the Drosophila wing are differentially organized by the fat/dachsous pathway. *PLOS Genetics*, 7(2), e1001305. https://doi.org/10.1371/journal.pgen.1001305.

Houle, D., Mezey, J., Galpern, P., & Carter, A. (2003). Automated measurement of Drosophila wings. *BMC Evolutionary Biology*, 3(1), 25. https://doi.org/10.1186/1471-2148-3-25.

Hwang, S., Song, S., Hong, Y. K., Choi, G., Suh, Y. S., Han, S. Y., Lee, M., Park, S. H., Lee, J. H., Lee, S., Bang, S. M., Jeong, Y., Chung, W.-J., Lee, I.-S., Jeong, G., Chung, J., & Cho, K. S. (2013). Drosophila DJ-1 decreases neural sensitivity to stress by negatively regulating Daxx-like protein through dFOXO. *PLoS Genetics*, 9(4), e1003412. https://doi.org/10.1371/journal.pgen.1003412.

Jennings, M. D., Blankley, R. T., Baron, M., Golovanov, A. P., & Avis, J. M. (2007). Specificity and autoregulation of notch binding by tandem WW domains in suppressor of deltex. *The Journal of Biological Chemistry*, 282(39), 29032–29042. https://doi.org/10.1074/jbc.M703453200.

Jiggins, C. D. (2016). *The ecology and evolution of heliconius butterflies*. Oxford University Press.

Jiggins, C. D., Salazar, P. A., & Montejo-Kovacevich, G. (2019). *Heliconiine butterfly collection records from University of Cambridge*. Department of Zoology. https://doi.org/10.15468/qabb9f.

Jones, R. T., Poul, Y. L., Whibley, A. C., Mérot, C., ffrench-Constant, R. H., & Joron, M. (2013). Wing shape variation associated with mimicry in butterflies. *Evolution*, 67(8), 2323–2334. https://doi.org/10.1111/evo.12114.

Kopelman, N. M., Mayzel, J., Jakobsson, M., Rosenberg, N. A., & Mayrose, I. (2015). CLUMPAK: A program for identifying clustering modes and packaging population structure inferences across K. *Molecular Ecology Resources*, 15(5), 1179–1191.

Korneliussen, T. S., Albrechtsen, A., & Nielsen, R. (2014). ANGSD: Analysis of next generation sequencing data. *BMC Bioinformatics*, 15(1), 356. https://doi.org/10.1186/s12859-014-0356-4.

Kozak, K. M., Wahlberg, N., Neild, A. F. E., Dasmahapatra, K. K., Mallet, J., & Jiggins, C. D. (2015). Multilocus species trees show the recent adaptive radiation of the mimetic heliconius butterflies. *Systematic Biology*, 64(3), 505–524. https://doi.org/10.1093/sysbio/syv007.

Kuznetsova, A., Brockhoff, P. B., & Christensen, R. H. B. (2017). lmerTest Package: Tests in linear mixed effects models. *Journal of Statistical Software*. https://doi.org/10.18637/jss.v082.i13.

Le Roy, C., Debat, V., & Llaurens, V. (2019a). Adaptive evolution of butterfly wing shape: From morphology to behaviour. *Biological Reviews*. https://doi.org/10.1111/brv.12500.

Le Roy, C., Debat, V., & Llaurens, V. (2019b). Adaptive evolution of butterfly wing shape: From morphology to behaviour. *Biological Reviews*. https://doi.org/10.1111/brv.12500.

Lewis, J. J., Geltman, R. C., Pollak, P. C., Rondem, K. E., Van Belleghem, S. M., Hubisz, M. J., Munn, P. R., Zhang, L., Benson, C., Mazo-Vargas, A., Danko, C. G., Counterman, B. A., Papa, R., & Reed, R. D. (2019). Parallel evolution of ancient, pleiotropic enhancers underlies butterfly wing pattern mimicry. *Proceedings of the National Academy of Sciences*, 116(48), 24174–24183. https://doi.org/10.1073/pnas.1907068116.

Li, B., Bickel, R. D., Parker, B. J., Saleh Ziabari, O., Liu, F., Vellichirammal, N. N., Simon, J.-C., Stern, D. L., & Brisson, J. A. (2020). A large genomic insertion containing a duplicated follistatin gene is linked to the pea aphid male wing dimorphism. *eLife*, 9, e50608. https://doi.org/10.7554/eLife.50608.

Li, T., Bellen, H. J., & Groves, A. K. (2018). Using Drosophila to study mechanisms of hereditary hearing loss. *Disease Models & Mechanisms*, 11(6), https://doi.org/10.1242/dmm.031492.

Lunde, K., Trimble, J. L., Guichard, A., Guss, K. A., Nauber, U., & Bier, E. (2003). Activation of the knirps locus links patterning to morphogenesis of the second wing vein in Drosophila. *Development*, 130(2), 235–248. https://doi.org/10.1242/dev.00207.

Mao, Y., Kucuk, B., & Irvine, K. D. (2009). Drosophila lowfat, a novel modulator of Fat signaling. *Development*, 136(19), 3223–3233. https://doi.org/10.1242/dev.036152.

Marees, A. T., de Kluiver, H., Stringer, S., Vorspan, F., Curis, E., Marie-Claire, C., & Derks, E. M. (2018). A tutorial on conducting genome-wide association studies: Quality control and statistical analysis. *International Journal of Methods in Psychiatric Research*, 27(2), e1608. https://doi.org/10.1002/mpr.1608.

Mazaleyrat, S. L., Fostier, M., Wilkin, M. B., Aslam, H., Evans, D. A. P., Cornell, M., & Baron, M. (2003). Down-regulation of notch target gene expression by suppressor of deltex. *Developmental Biology*, 255(2), 363–372. https://doi.org/10.1016/S0012-1606(02)00086-6.

McCulloch, G. A., Foster, B. J., Dutoit, L., Ingram, T., Hay, E., Veale, A. J., Dearden, P. K., & Waters, J. M. (2019). Ecological gradients drive insect wing loss and speciation: The role of the alpine treeline. *Molecular Ecology*, 28(13), 3141–3150. https://doi.org/10.1111/mec.15114.

Meier, J. I., Salazar, P. A., Kučka, M., Davies, R. W., Dréau, A., Aldás, I., Power, O. B., Nadeau, N. J., Bridle, J. R., Rolian, C., McMillan, O. W., Jiggins, C. D., & Chan, Y. F. (2021). Haplotype tagging reveals parallel formation of hybrid races in two butterfly species. *Proceedings of the National Academy of Sciences of the United States of America*. https://doi.org/10.1073/pnas.2015005118.

Mena, S., Kozak, K. M., Cárdenas, R. E., & Checa, M. F. (2020). Forest stratification shapes allometry and flight morphology of tropical butterflies. *Proceedings of the Royal Society B: Biological Sciences*, 287(1937), 20201071. https://doi.org/10.1098/rspb.2020.1071.

Mérot, C., Oomen, R. A., Tigano, A., & Wellenreuther, M. (2020). A roadmap for understanding the evolutionary significance of structural genomic variation. *Trends in Ecology & Evolution*, 35(7), 561–572. https://doi.org/10.1016/j.tree.2020.03.002.

Montejo-Kovacevich, G., Smith, J. E., Meier, J. I., Bacquet, C. N., Whiltshire-Romero, E., Nadeau, N. J., & Jiggins, C. D. (2019). Altitude and life-history shape the evolution of Heliconius wings. *Evolution*, 73(12), 2436–2450. https://doi.org/10.1111/evo.13865.

Nadeau, N. J., Ruiz, M., Salazar, P., Counterman, B., Medina, J. A., Ortiz-Zuazaga, H., Morrison, A., McMillan, W. O., Jiggins, C. D., & Papa, R. (2014). Population genomics of parallel hybrid zones in the mimetic butterflies, H. melpomene and H. erato. *Genome research*, 24(8), 1316–1333.

Nakagawa, S., Johnson, P. C. D., & Schielzeth, H. (2017). The coefficient of determination R2 and intra-class correlation coefficient from generalized linear mixed-effects models revisited and expanded. *Journal of the Royal Society Interface*, 14(134), 20170213. https://doi.org/10.1098/rsif.2017.0213.

Pan, B.-Y., Liu, Y.-K., Wu, H.-K., Pang, X.-Q., Wang, S.-G., Tang, B., & Xu, C.-D. (2020). Role of phosphoglucomutase in regulating trehalose metabolism in Nilaparvata lugens. *3 Biotech*, 10(2), 61. https://doi.org/10.1007/s13205-020-2053-5.

Pardo-Diaz, C., Salazar, C., & Jiggins, C. D. (2015). Towards the identification of the loci of adaptive evolution. *Methods in Ecology and Evolution*, *6*(4), 445–464. https://doi.org/10.1111/2041-210X.12324.

Pitchers, W., Nye, J., Márquez, E. J., Kowalski, A., Dworkin, I., & Houle, D. (2019). A multivariate genome-wide association study of wing shape in *Drosophila melanogaster*. *Genetics*, *211*(4), 1429–1447. https://doi.org/10.1534/genetics.118.301342.

R Development Core Team (2011). *A language and environment for statistical computing*, Vienna: R Foundation for Statistical Computing. http://www.R-project.org.

Schindelin, J., Arganda-Carreras, I., Frise, E., Kaynig, V., Longair, M., Pietzsch, T., & Cardona, A. (2012). Fiji: an open-source platform for biological-image analysis. *Nature methods*, *9*(7), 676–682.

Shamloula, H. K., Mbogho, M. P., Pimentel, A. C., Chrzanowska-Lightowlers, Z. M. A., Hyatt, V., Okano, H., & Venkatesh, T. R. (2002). Rugose (rg), a Drosophila A kinase anchor protein, is required for retinal pattern formation and interacts genetically with multiple signaling pathways. *Genetics*, *161*(2), 693–710.

Skotte, L., Korneliussen, T. S., & Albrechtsen, A. (2012). Association testing for next-generation sequencing data using score statistics. *Genetic Epidemiology*, *36*(5), 430–437. https://doi.org/10.1002/gepi.21636.

Skotte, L., Korneliussen, T. S., & Albrechtsen, A. (2013). Estimating individual admixture proportions from next generation sequencing data. *Genetics*, *195*(3), 693–702. https://doi.org/10.1534/genetics.113.154138.

Song, Y.-H., Mirey, G., Betson, M., Haber, D. A., & Settleman, J. (2004). The Drosophila ATM Ortholog, dATM, Mediates the response to ionizing radiation and to spontaneous DNA damage during development. *Current Biology*, *14*(15), 1354–1359. https://doi.org/10.1016/j.cub.2004.06.064.

Stoffel, M. A., Nakagawa, S., & Schielzeth, H. (2017). RptR: repeatability estimation and variance decomposition by generalized linear mixed-effects models. *Methods in Ecology and Evolution*, *8*(11), 1639–1644. https://doi.org/10.1111/2041-210X.12797.

Strauss, R. E. (1990). Patterns of quantitative variation in Lepidopteran wing morphology: The convergent groups Heliconiinae and Ithomiinae (PAPILIONOIDEA: NYMPHALIDAE). *Evolution*, *44*(1), 86–103. https://doi.org/10.1111/j.1558-5646.1990.tb04281.x.

Szpiech, Z. A., & Hernandez, R. D. (2014). selscan: An efficient multi-threaded program to perform EHH-based scans for positive selection. *Molecular Biology and Evolution*, *31*(10), 2824–2827. https://doi.org/10.1093/molbev/msu211.

Tavares, H. (2020). *Tavareshugo/WindowScanR [R]*. Retrieved from https://github.com/tavareshugo/WindowScanR (Original work published 2016).

Thomas, M. A., Walsh, K. A., Wolf, M. R., McPheron, B. A., & Marden, J. H. (2000). Molecular phylogenetic analysis of evolutionary trends in stonefly wing structure and locomotor behavior. *Proceedings of the National Academy of Sciences*, *97*(24), 13178–13183. https://doi.org/10.1073/pnas.230296997.

Thurmond, J., Goodman, J. L., Strelets, V. B., Attrill, H., Gramates, L. S., Marygold, S. J., Matthews, B. B., Millburn, G., Antonazzo, G., Trovisco, V., Kaufman, T. C., Calvi, B. R., Perrimon, N., Gelbart, S. R., Agapite, J., Broll, K., Crosby, L., Santos, G. D., Emmert, D., … Baker, P. (2019). FLYBASE 2.0: The next generation. *Nucleic Acids Research*, *47*(D1), D759–D765. https://doi.org/10.1093/nar/gky1003.

Tigano, A., & Friesen, V. L. (2016). Genomics of local adaptation with gene flow. *Molecular Ecology*, *25*(10), 2144–2164. https://doi.org/10.1111/mec.13606.

Van Belleghem, S. M., Rastas, P., Papanicolaou, A., Martin, S. H., Arias, C. F., Supple, M. A., Hanly, J. J., Mallet, J., Lewis, J. J., Hines, H. M., Ruiz, M., Salazar, C., Linares, M., Moreira, G. R. P., Jiggins, C. D.,

Counterman, B. A., McMillan, W. O., & Papa, R. (2017). Complex modular architecture around a simple toolkit of wing pattern genes. *Nature Ecology & Evolution*, *1*, https://doi.org/10.1038/s41559-016-0052.

Volders, K., Scholz, S., Slabbaert, J. R., Nagel, A. C., Verstreken, P., Creemers, J. W. M., Callaerts, P., & Schwarzel, M. (2012). Drosophila rugose Is a functional homolog of mammalian neurobeachin and affects synaptic architecture, brain morphology, and associative learning. *Journal of Neuroscience*, *32*(43), 15193–15204. https://doi.org/10.1523/JNEUROSCI.6424-11.2012.

Wang, N., Leung, H.-T., Mazalouskas, M. D., Watkins, G. R., Gomez, R. J., & Wadzinski, B. E. (2012). Essential roles of the Tap42-regulated protein phosphatase 2A (PP2A) family in wing imaginal disc development of *Drosophila melanogaster*. *PLoS One*, *7*(6), e38569. https://doi.org/10.1371/journal.pone.0038569.

Wilkin, M. B., Carbery, A.-M., Fostier, M., Aslam, H., Mazaleyrat, S. L., Higgs, J., Myat, A., Evans, D. A. P., Cornell, M., & Baron, M. (2004). Regulation of notch endosomal sorting and signaling by Drosophila Nedd4 family proteins. *Current Biology*, *14*(24), 2237–2244. https://doi.org/10.1016/j.cub.2004.11.030.

Wise, A., Tenezaca, L., Fernandez, R. W., Schatoff, E., Flores, J., Ueda, A., & Venkatesh, T. (2015). Drosophila mutants of the autism candidate gene neurobeachin (rugose) exhibit neuro-developmental disorders, aberrant synaptic properties, altered locomotion, and impaired adult social behavior and activity patterns. *Journal of Neurogenetics*, *29*(2–3), 135–143. https://doi.org/10.3109/01677063.2015.1064916.

Wootton, R. (2002). Functional morphology of insect wings. *Annual Review of Entomology*, https://doi.org/10.1146/annurev.ento.37.1.113.

Wu, C., Chakrabarty, S., Jin, M., Liu, K., & Xiao, Y. (2019). Insect ATP-Binding Cassette (ABC) transporters: Roles in xenobiotic detoxification and Bt insecticidal activity. *International Journal of Molecular Sciences*, *20*(11), 2829. https://doi.org/10.3390/ijms20112829.

Yeaman, S. (2015). Local adaptation by alleles of small effect. *The American Naturalist*, *186*(S1), S74–S89. https://doi.org/10.1086/682405.

Zhao, J., Lu, Y., Zhao, X., Yao, X., Shuai, Y., Huang, C., & Zhong, Y. (2013). Dissociation of rugose-dependent short-term memory component from memory consolidation in Drosophila. *Genes, Brain, and Behavior*, *12*(6), 626–632. https://doi.org/10.1111/gbb.12056.

Zhou, X., St. Pierre, C. L., Gonzales, N. M., Zou, J., Cheng, R., Chitre, A. S., Sokoloff, G., & Palmer, A. A. (2020). Genome-wide association study in two cohorts from a multi-generational mouse advanced intercross line highlights the difficulty of replication due to study-specific heterogeneity. *G3: Genes, Genomes, Genetics*, *10*(3), 951–965. https://doi.org/10.1534/g3.119.400763.

Zuur, A., Ieno, E. N., Walker, N., Saveliev, A. A., & Smith, G. M. (2009). *Mixed effects models and extensions in ecology with R*. Springer Science & Business Media.

SUPPORTING INFORMATION

Additional supporting information may be found online in the Supporting Information section.